

**A GPR POLARIZATION EXPERIMENT
ON STORGLACIÄREN**

Ariane Heinz-Vallribera

Submitted to the *Arctic Centre* on July 8, 2003

A GPR Polarization Experiment on Storglaciären

Ariane Heinz-Vallribera

ABSTRACT

Ground Penetrating Radar has been used for many years to study the internal structure of glaciers and has proved to be an excellent tool. Polarization is an important consideration when designing a GPR survey strategy because most GPR antennas are dipoles that radiate linearly polarized waves and are sensitive to the polarization of waves reflected from buried targets, and because some targets reflect waves preferentially depending on the polarization of the incident wave.

In this report, the polarization scattering properties of two important GPR targets, the flat plane and the long circular cylinder, as well as their analogies in glaciology, are compared and contrasted. Following this, a modest GPR polarization experiment conducted during the GlacioEuroLab5 winter course on Storglaciären, a small valley glacier in northern Sweden, is presented and discussed.

Knowledge of the depolarizing properties of specific targets or sources of clutter may be used to design the optimal GPR antenna configuration for a specific study. Does the same apply to glacial studies?

Introduction

Radar is known to be an excellent tool to study the internal structure of glaciers and has been used for this purpose since the 1950s. Different types of studies are typically conducted, including mapping the bedrock beneath glaciers and ice sheets, analyzing the most relevant layers of firn and ice, determining snow accumulation rates for mass balance studies, or mapping outstanding features such as crevasses, moulins, melt-water tunnels and other subglacial drainage system features.

One of the keys to success in GPR studies is using the most appropriate equipment for each specific survey goal. One needs to know the limitation of the equipment that is being used. For instance, low frequency antennas can achieve great depths of investigation (as long as the soil properties are favorable, of course) but may lack the resolution needed for identifying thin layers or small targets. If a high

resolution is needed, higher frequency antennas will have to be used.

Polarization is also a significant consideration in implementing a GPR study strategy, especially in heterogenous soils where it may be important to discriminate between reflections arriving from undesirable scatterers and from primary GPR targets. In this paper we will try to see how important the polarization factor may be for optimizing potential detection of glaciology features.

Theoretical background

When electromagnetic waves are propagating through a host medium, scattering from contrasts in intrinsic impedance occurs. The size, shape, composition and orientation of the scatterer relative to the incident electromagnetic field determine the polarization characteristics of the scattered field.

As illustrated in Figure 1, a dipole GPR antenna radiates linearly polarized waves, and the majority of the radiated electric field contains vector components oriented parallel to the long axis of the transmitting antenna. The distribution of the radiated fields is dependent on the soil properties, and buried targets may reflect depolarized waves. Finally, the receiving antenna is sensitive to the polarization of waves incident on its surface. The polarization sensitivity of a particular antenna configuration depends on the relative position of the transmitting and receiving antennas, the field patterns of the antennas, and the depolarization properties of the scatterer.

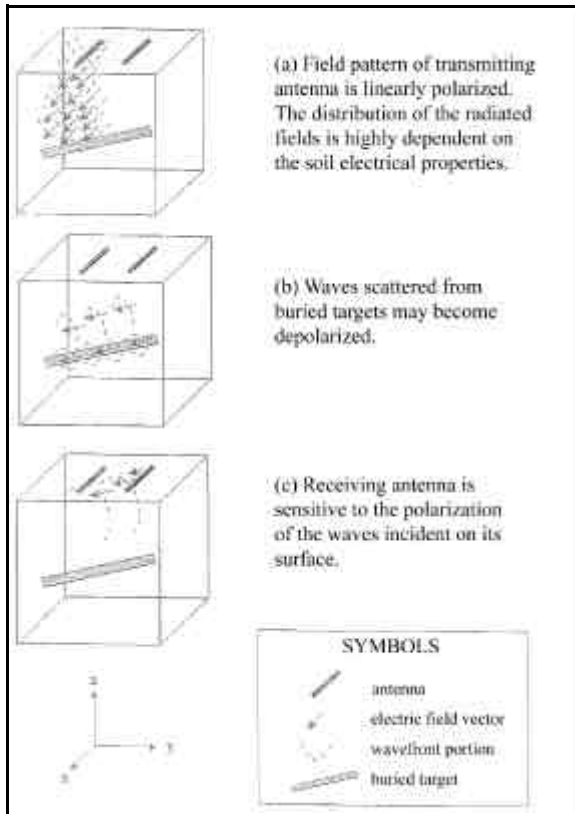


Figure 1. Diagrams showing the major facets of GPR polarization phenomena (modified from Roberts and Daniels, 1996).

Roberts (1994) introduces the concept of scattering polarization loss factor (SPLF) to describe the polarization properties of a specific GPR arrangement. The SPLF is defined as follows:

$$SPLF = (\hat{e}^i \cdot \hat{e}^r)^2 \quad (1)$$

where \hat{e}^i is the incident unit polarization vector and \hat{e}^r is the scattered unit polarization vector. These vectors, as well as their decomposition into perpendicular \hat{e}_\perp and parallel components $\hat{e}_{\parallel ta}$, are shown in Figure 2.

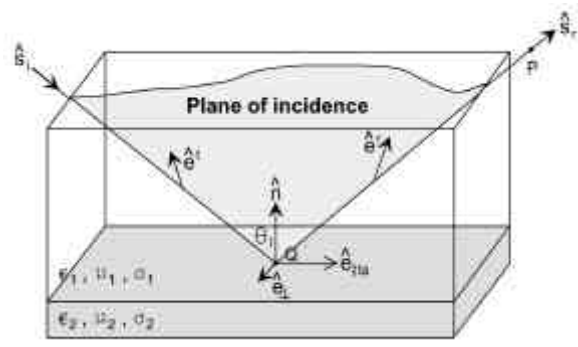


Figure 2. Coordinate reference frame for decomposition of incident and reflected polarization vectors into orthogonal components (modified from Roberts and Daniels, 1996).

The SPLF is zero (total depolarization) when the polarization of the scattered wave is orthogonal to the polarization of the incident wave, one-half when the angle formed by the incident and scattered polarization vectors is 45 degrees, and one (no depolarization) when the incident and scattered waves have identical polarizations.

In a paper published in the *Journal of Environmental and Engineering Geophysics*, Roberts and Daniels investigate with more detail two particular cases: 1) scattering from planar interfaces and 2) scattering from long circular cylinders. They introduce the E_y/E_x scattered-to-incident polarization ratio ($SIPR_{yx}$) defined as:

$$SIPR_{yx} = \frac{\frac{E_y^s}{E_x^s}}{\frac{E_y^i}{E_x^i}} \quad (2)$$

which value is indicative of the polarization state of the reflected field:

$$\begin{aligned} |SIPR_{yx}| < 1 &\Rightarrow E_x \text{ preferentially reflected.} \\ |SIPR_{yx}| = 1 &\Rightarrow \text{No polarization sensitivity.} \\ |SIPR_{yx}| < 1 &\Rightarrow E_y \text{ preferentially reflected.} \end{aligned}$$

The $SIPR_{yx}$ can also be written as (Robert and Daniels, 1996):

$$SIPR_{yx} = \frac{\frac{E_x^i S_{xy} + E_z^i S_{zy} + E_y^i S_{yy}}{E_y^i}}{\frac{E_y^i S_{yx} + E_z^i S_{zx} + E_x^i S_{xx}}{E_x^i}} \quad (3)$$

where S_{ij} ($i, j = x, y, z$) are scattering coefficients.

1) Scattering from planar interfaces

The polarization of the scattered field from planar interfaces can be predicted through vector computations involving Fresnel's

equations and Snell's laws. In terms of the geometry of bistatic GPR configurations, Roberts and Daniels (1996) observe that very little of the scattered energy from planar reflectors arriving at the receiving antenna is depolarized if the incident angle θ_i is less than 20 degrees.

Several transmitting/receiving antenna configurations with different types of planar reflectors are presented in Figure 3.

2) Scattering from long circular cylinders

The scattered fields from infinite length circular cylinders for plane wave incidence can be calculated from the exact series solution (Roberts and Daniels, 1996; Ruck and others, 1970; Wait, 1955). Unlike planar surfaces, they may be strongly depolarized at low angles of incidence because the scattering coefficients of the parallel and perpendicular components of the incident field are not equal.

Figure 4 displays graphs of the bistatic

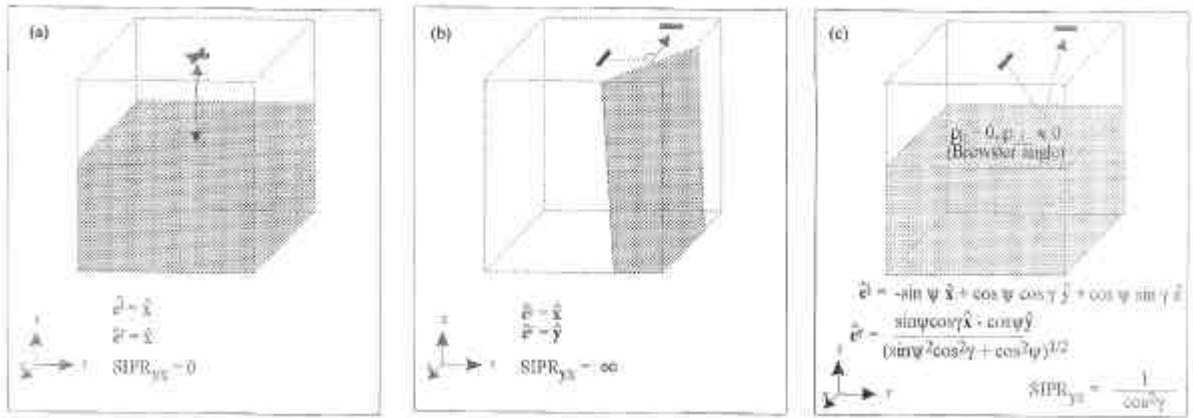


Figure 3. Illustrations of various $SIPR_{yx}$ for reflections from planar interfaces, assuming far field conditions (from Roberts and Daniels, 1996)

(a) shows the case of a crossed dipole with one arm transmitting and the other arm receiving the reflected field from a horizontal plane, with a $SIPR_{yx}$ equal to 0. The $SIPR_{yx}$ is never greater than 1 when coincident transmitting under achievers are used and the scatterer is a flat plane because the back-scattered field from a plane is never depolarized.

(b) presents an instance where $SIPR_{yx}$ is greater than 1 due to polarization associated with S_{xy} . The incident field is primarily parallel-polarized and the angle of incidence θ_i is 45 degrees.

In (c), the interface is penetrable and the medium below the interface possesses a lower intrinsic impedance than the medium above the interface. The perpendicular-polarized component is preferentially reflected relative to the parallel-polarized component. For the antennas positioned as shown in the figure, the fields are incident on the interface at the Brewster angle and the $SIPR_{yx}$ is greater than 1.

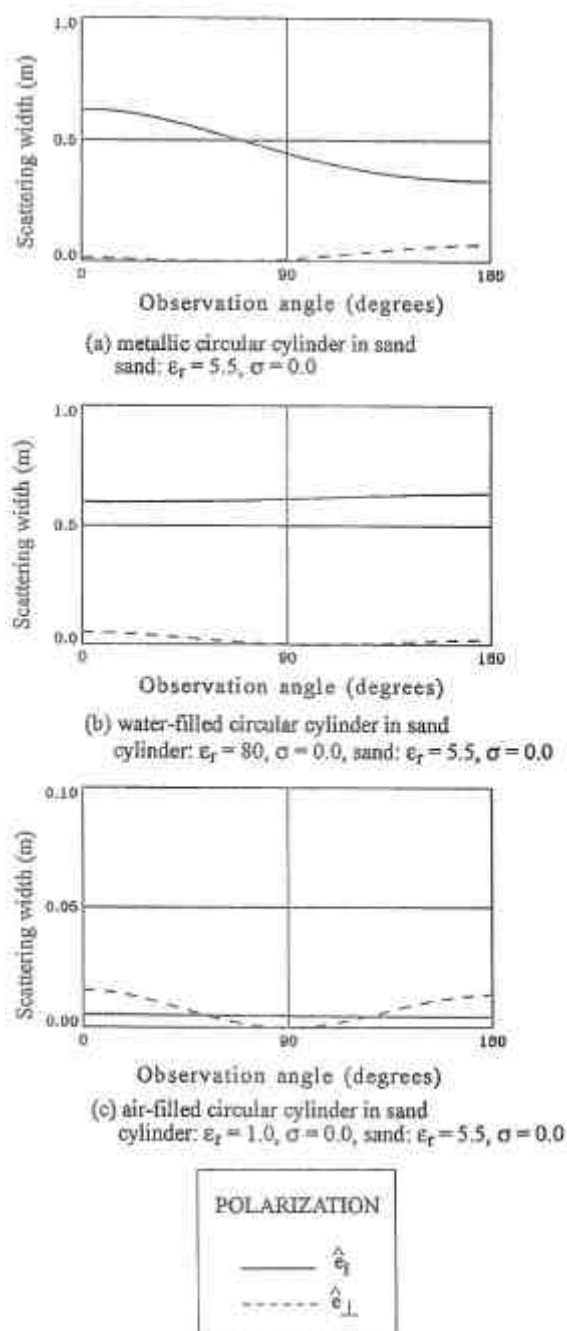


Figure 4. Scattering widths versus observation angle of $0.0625 a/\lambda$ cylinders of differing compositions, calculated using the exact series solution (from Roberts and Daniels, 1996).

scattering widths of small-diameter (radius / incident wavelength ratio $a/\lambda=0.0625$) pipes.

There is a significant difference in \hat{e}_{\parallel} and \hat{e}_{\perp} scattering widths associated with scattering from metallic and low-velocity cylinders. For all observation angles, the scattered fields are

depolarized when the incident energy contains \hat{e}_{\parallel} and \hat{e}_{\perp} components, and most efficient when the incident polarization is parallel to the long axis of the cylinder. In contrast, with air-filled (or high-velocity) cylinders, the amplitudes of scattered \hat{e}_{\parallel} and \hat{e}_{\perp} components with observation angles near 45 degrees are equivalent, and the scattered fields are not depolarized.

Recommended GPR configurations and application to Glaciology

The most desirable GPR strategy in most cases would involve the collection of data in an orthogonal grid pattern. This allows the creation of a 3-D image in which estimates of target geometries can be made. Also, problems associated with side-reflections, a concern when interpreting single profile lines, are alleviated.

Collecting multiple polarization data is another alternative, especially when a grid pattern is not an option. As an example, Figure 5 presents multiple polarization data obtained along a profile line oriented 45 degrees relative to a pipe and horizontally offset 0.5 m from a sphere buried 0.5 m in clean sand. The strong cross-polarized and parallel-polarized scattering from the pipe infer its presence and possibly its identity, whereas the weak cross-polarized signal from the sphere and the fact that it switches polarity across the profile would indicate the presence of an offset from the profile line.

The two following antenna arrangements are the most commonly utilized.

Parallel-polarized antennas. This bistatic antenna arrangement, also known as the (||) mode, is the most commonly utilized and has the transmitting and receiving antennas oriented parallel to each other and perpendicular to the direction of motion. This configuration is the most sensitive to buried

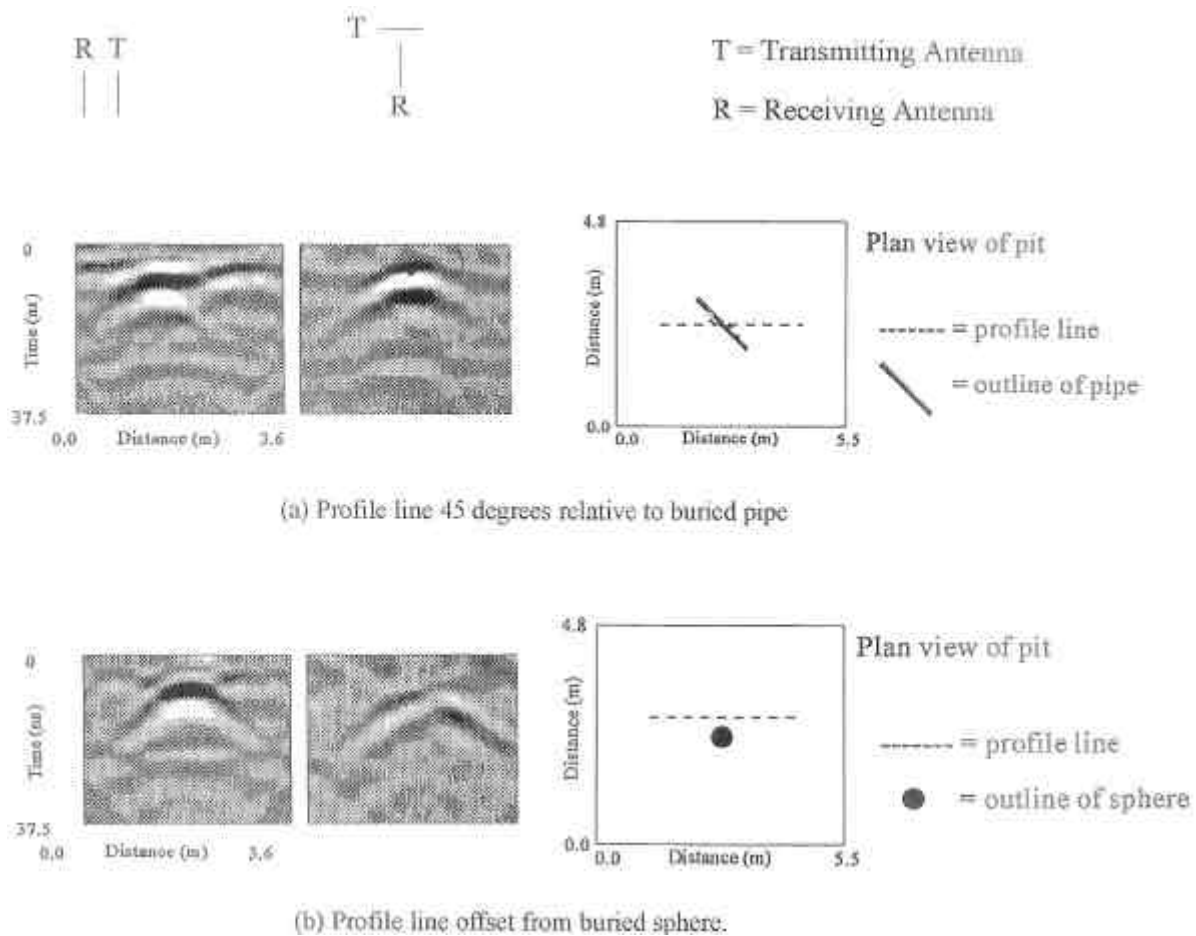


Figure 5. Comparison of multiple polarization data collected along profile lines: (a) 45 degrees relative to a 1.6 m length and 0.05 m diameter metallic pipe buried 0.5 m in slightly moist sand, and (b) horizontally offset 0.45 m from a 0.05 m diameter sphere buried 0.5 m in slightly moist sand (from Roberts and Daniels, 1996).

targets such as horizontal interfaces and low-velocity cylinders oriented parallel to the long axes of the antennas, but is relatively insensitive to depolarized scattered fields.

In glaciology, this would be the most appropriate setup for mapping **snow, firn and/or ice layers**, as well as the **bedrock beneath the ice sheet**, provided that their orientation is relatively horizontal. For dipping layers, positioning the long axes of the antennas parallel to the strike of the layer will produce the strongest reflection strength because it will ensure that the greatest portion of the incident energy is perpendicular-polarized. One way to determine the strike of a dipping layer is by rotating a (I) pair of antennas around a circle and examining the variation in the reflection strength versus

rotation angle.

This (I) configuration should also be the most appropriate for locating **meltwater streams** when they are oriented approximately parallel to the long axis of the antennas. In contrast, the optimum configuration for finding **ice caves or tunnels** will be the (–) mode (long axes of antennas parallel to direction of motion, and perpendicular to cave or other long cylindrical target) because long high-velocity cylinders scatter incident waves most efficiently when the incident polarization is perpendicular to the long axis of the cylinder.

Cross-polarized antennas. The most advantageous position for the cross-polarized receiving antenna is across the transmitting antenna, at an angle of approximately 90

degrees. This angle will maximize the potential for detecting depolarized fields scattered from long cylindrical features and minimize the reflection strength from non-depolarizing features such as planar reflectors. There is, however, a risk of non-detection due to symmetry if the transmitting antenna and the feature are oriented parallel to each other. An angle of 45 degrees would be sensitive to both planar reflectors and strong depolarizing features, which would not be an advantage when trying to discriminate between different types of reflectors.

In glaciology, this type of configuration also known as (\perp) mode, would possibly be the most appropriate when trying to map depolarizing features such as **meltwater streams, ice caves, tunnels, crevasses, and others**, because they would be positively discriminated from other reflections in the GPR data.

Description of experiment

A modest GPR polarization experiment was conducted in the ablation area of Storglaciären, a small valley glacier in the Kebnekaise range (northern Sweden) on March 31st 2003, with the resources left from a previous more ambitious GPR/GPS skidoo survey for measuring ice thickness in the area. A commercial RAMAC GPR device (Malå Geoscience, Sweden), operating with two unshielded 200 MHz dipole antennas, was used. The two antennas were mounted on a plastic sled, which was being pulled by a scientist who was also carrying the control unit, while the radar operator was walking next to it controlling the data collection with a laptop computer. Figure 6 is a picture taken during the survey.

Two different antenna arrangements were used and are presented on Figure 7. Setup 1 corresponds to the (\parallel) mode explained in the previous section, with two antennas parallel to



Figure 6. GPR polarization survey conducted on March 31st 2003 in the ablation area of Storglaciären. A commercial RAMAC GPR device (Malå Geoscience, Sweden) operating with two unshielded 200 MHz dipole antennas mounted on a plastic sled were used. A scientist was pulling the plastic sled while the radar operator was controlling the data collection with a laptop. Photograph courtesy of Fay Campbell.

each other, perpendicular to the direction of motion, and separated 45 cm apart, while Setup 2 corresponds to the (\perp) mode, with the transmitting antenna in the same position and the receiving antenna perpendicular to it, with a separation of 37 cm between centers. A third angle experiment according to the (\ominus) mode was planned but could not be carried out due to insufficient computer battery life.

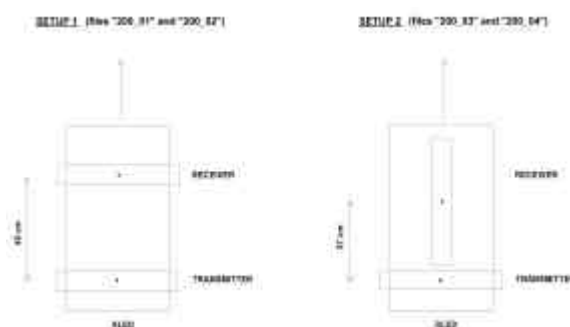


Figure 7. GPR antenna configurations. Setup 1 corresponds to the (\parallel) mode, and Setup 2 to the (\perp) mode.

One profile was collected for each antenna configuration along the same line oriented

approximately in the east-west direction. The data collection was triggered on time, with the sled being pulled at a relatively constant walking speed. The profile obtained with Setup 1 is presented in Appendix A and the profile obtained with Setup 2, in Appendix B.

Discussion

No major conclusions can be drawn from the two radar profiles. No small outstanding targets, which are more likely to be polarization-sensitive, can be recognized. Several large reflectors can be identified, and generally appear stronger in the profile corresponding to Setup 1, especially at shallow depths. Below 20 meters, there doesn't seem to be any preferential configuration; some of the reflectors appear slightly stronger in one profile or the other, but they can still be easily identified in any case.

Conclusions

The most desirable GPR study would be the collection of multiple profiles in a grid pattern, which would enable the creation of a 3-D image of the glacier. However, GPR data collection in inhospitable environments such as glaciers is not an insignificant task. It can take days or even weeks of waiting time to be able to access the areas to be surveyed. It may be difficult to establish a good and lasting survey grid which would allow multiple surveying with different antenna arrangements. Therefore, it is important to plan all the survey details, such as what kind of antenna arrangement to use to best meet the goals of the survey, thus taking advantage of what may be only a day or two of cooperative weather.

The GPR polarization experiment conducted on Storglaciären is not conclusive in one way or another. The two sets of data are certainly different, but it would be hazardous to draw any conclusions from these two profiles. It would be interesting to carry out some more

complete polarization experiments on well-studied glaciers in order to try to establish a well-working methodology that would facilitate the decision on which GPR strategy to use for each specific goal.

References

Maijala, P., Moore, J.C., and others, GPR Investigations of Glaciers and Sea Ice in the Scandinavian Arctic.

Moore, J.C., Kohler, J., Isaksson, E., Maijala, P. Comparison of modelled and observed responses of a glacier snowpack to ground-penetrating radar, *Annals of Glaciology*, 37, in press, 2003.

Roberts, R.L., Daniels, J.D., Analysis of GPR polarization phenomena, *Journal of Environmental and Engineering Geophysics*, Vol. 1, No. 2, 1996.

Ruck, G.T., Barrick, D.E., Stuart, W.D., and Krichbaum, C.K., Radar Cross Section Handbook, Vol. I, *Plenum Press*, 1970.

Stratton, J.A., Electromagnetic Theory, *McGraw Hill*, 1941.

Sugden, D.E., and John, B.S., Glaciers and Landscape, *Edward Arnold*, 1977.

Wait, J.R., Scattering of a plane wave from a circular dielectric cylinder at oblique incidence, *Canad. J. Phys.*, 33, 1955.

Acknowledgments

I would like to thank the European Union for funding courses like GlacioEuroLab, as well as the educators, participants and staff at Tarfala Research Station for their kindness and professionalism.

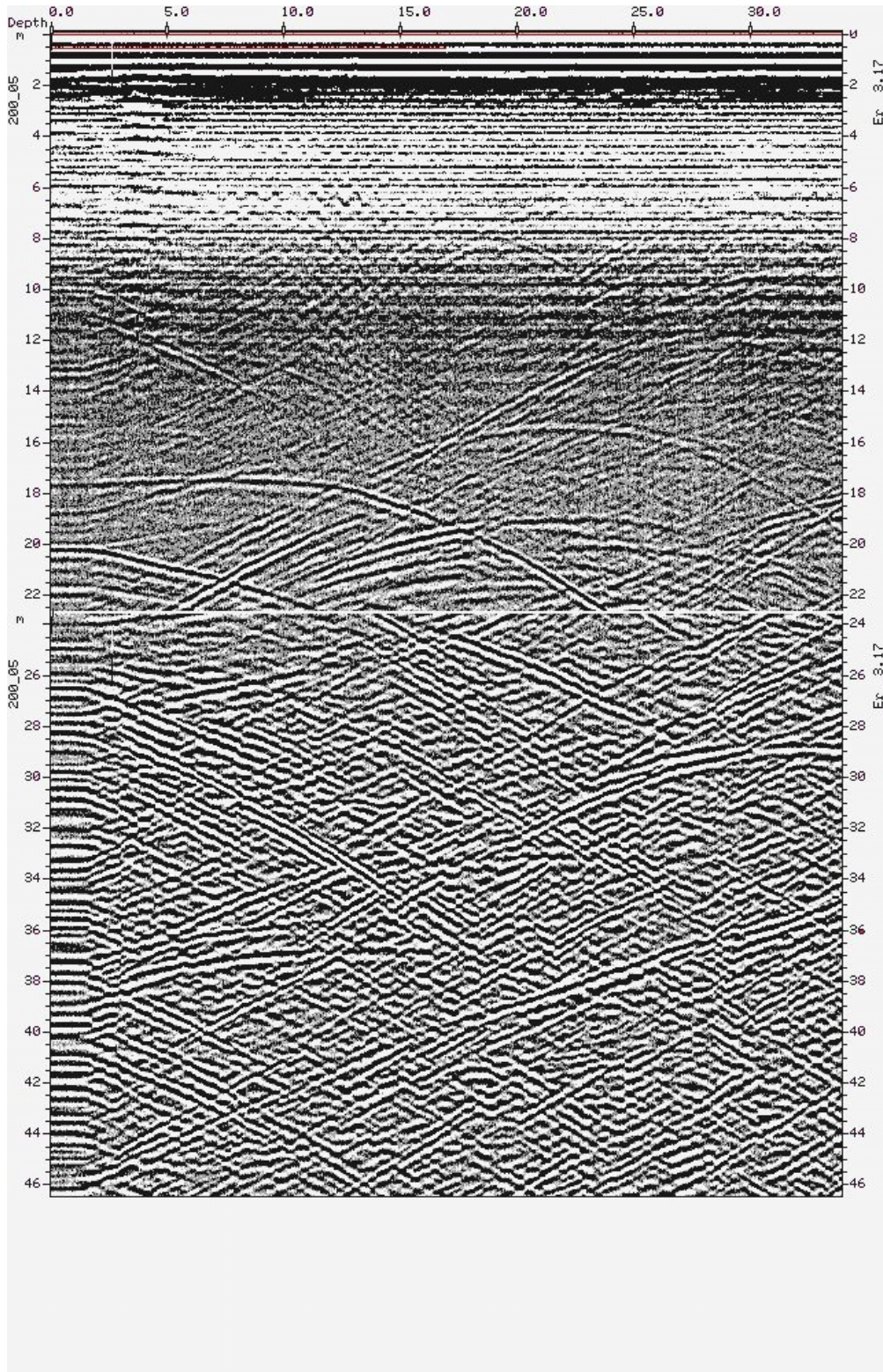
Very special thanks also to Roger Roberts for sparing some of his busy time and letting me

gain access to lots of very useful literature, including his own.

Finally, I would like to thank my employer Doria Kutrubes for her encouragement and financial assistance.

APPENDIX A

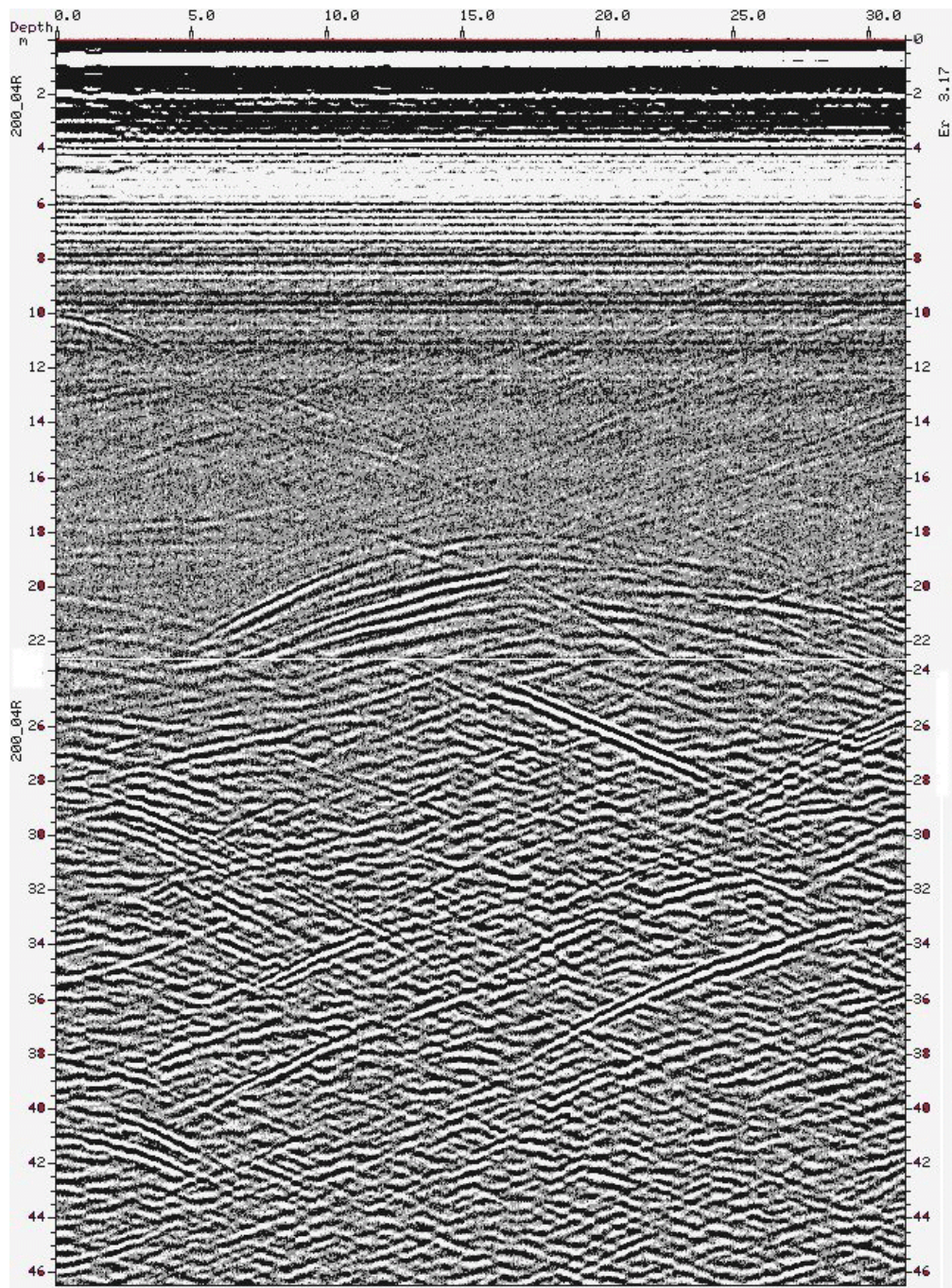
GPR profile for Setup 1 - (I) mode



GPR profile for Setup 1. The horizontal scale is in meters, and the vertical scale is in meters calculated with a dielectric permittivity of 3.17 (ice). Digital processing of image, including DC-level removal, handled by Anna Sinisalo.

APPENDIX B

GPR profile for Setup 2 - (\perp) mode



GPR profile for Setup 2. The horizontal scale is in meters, and the vertical scale is in meters calculated with a dielectric permittivity of 3.17 (ice). Digital processing of image, including DC-level removal, handled by Anna Sinisalo.